J. Min. Metall. Sect. B-Metall. 50 (2) B (2014) 133 - 137

Journal of Mining and Metallurgy, Section B: Metallurgy

EFFECT OF HEAT TREATMENT ON STRUCTURAL CHANGES IN METASTABLE AlSi10Mg ALLOY

B. Jordović, B. Nedeljković, N. Mitrović*, J. Živanić, A. Maričić

University of Kragujevac, Faculty of Technical Sciences Čačak, Čačak, Serbia

(Received 23 October 2012; accepted 07 July 2014)

Abstract

This paper presents a study on structural changes occurring in a rapidly quenched metastable AlSi10Mg alloy during heating cycles within the temperature range from room temperature to 800 K. Measurement of electrical resistivity of a ribbon showed that structural stabilization takes place at temperatures ranging from 450 K to 650 K. The isotherms of the electrical resistivity measured at temperatures 473 K, 483 K and 498 K revealed two stages of structural stabilization i.e. a kinetic process and diffusion process. Measurement of the thermoelectromotive force of the thermocouple made from the investigated alloy and a copper conductor by a mechanical joining was used to determine relative changes in the electron density of states of the quenched sample after successive heat treatments. The same alloy sample was subjected to successive heat treatments at temperatures up to 503 K, 643 K, 683 K and 763 K. The change in the thermopower suggested that each heating was followed by an increase in free electron density in the alloy. Therefore, the abrupt decline in electrical resistivity was induced by an increase in both the mean free electron path and free electron density during the thermal stabilization of the structure.

Keywords: Metastable AlSiMg alloy, Melt spinning, Thermoelectric properties, Structure relaxation

1. Introduction

Amorphous and nanostructured metallic alloys are among advanced materials with functional properties suitable for use in all technical fields [1], particularly electrical engineering [2]. These materials are commonly obtained by rapidly quenching of molten alloys consisting of transition metals (Fe, Ni, Co, Ti, Mo, Nb, V, Cr, Zr, Pd) - which determine functional (magnetic, mechanical and electrical) properties and metalloids (B, Si, P, C, Ge) - which are responsible for inhibition of crystallization during the hardening process. High cooling rates of about 10^6-10^8 K/s attained during melt-spinning enable atomic arrangement of less than 1 nm [3].

However, amorphous structure of the materials is structurally and thermodynamically unstable and highly susceptible to partial or complete crystallization during thermal treatment. Therefore, it requires knowledge of alloy stability at different temperatures. Generally speaking, stability refers to the thermally active transition from a metastable, disordered amorphous structure to an orderly arranged crystal structure. During synthesis of amorphous alloys, obtained by casting, special care should be taken regarding the proportion of components in the alloy, in order to achieve property improvement, such as enhanced glass-forming ability, good alloy castability (resulting in a good surface finish and high homogeneity of alloy ribbons) and improved thermal stability of the amorphous structure [4-6].

Intensive research into the kinetic properties of amorphous and nanocrystalline alloys suggests a correlation between the physical nature of the anomalous behaviour of the electron state density at the Fermi level, thermal conductivity, heat capacitance and electrical resistivity, as well as structural inhomogeneities of these materials [7-9]. During annealing of amorphous alloys at temperatures about 100 K lower than crystallization temperature, two competitive processes take place: free volume decreases, leading to a reduced rate of diffusion mass transport, and arrangement processes, which bring the alloy closer to the crystallized state and, hence, increase its readiness to crystallize. The thermoelectromotive force (TEMF) measurements of amorphous/metastable alloys can be successfully used for investigation of structural transformation during crystallization process [10].

The objective of this study was to evaluate the effect of structural changes of the metastable AlSi10Mg alloy during annealing on its thermoelectrical properties. The AlSi10Mg alloy is known as very well casting alloy with low density, good thermal properties and suitable mechanical properties [11]. Brandt and Neuer [12] reported

* *Corresponding author: nebojsa.mitrovic@ftn.kg.ac.rs*

DOI:10.2298/JMMB121023011J

measurements of the electrical resistivity of AlSiMg alloys with a systematic variation of Si content (5%, 7%, 9% and 12 % - consequently, increase of Si addition lead to the observed increase of electrical resistivity). Daoudi et al. investigated the non-isothermal kinetic parameters of the metastable phases (of an extruded AlSiMg alloy) obtained by water quenching of heated samples up to 573 K [13] or up to 813 K [14]. Those studies have detailed analysis of transformed fraction from metastable to stable phase. Isothermal study of AlSiMg commercial alloy (with low Si content – 0.5 wt. %) prepared by solution treatment at 823 K / 15 min followed by water quenching was performed using electrical resistivity measurements in the range 430-480 K [15]. However, there is a lack of the casting experiments of this alloy by melt spinning technique with cooling rate of about 10^5 K/s [16]. Just thermodynamic analysis of AlSi10Mg alloy samples prepared by mould casting up to cooling rate of 100 K/s was performed [17]. Furthermore, there is no data of the thermoelectromotive force of this typical casting material.

2. Experimental

Metastable AlSi10Mg alloy ribbons of 35-70 μm thickness and 1-3 mm width were studied. Table 1 presents the chemical composition of the casting alloy.

The ribbons were prepared by rapidly quenching of the molten alloy using the melt-spinning method at the Joint Laboratory for Advanced Materials of SASA, Section for Amorphous Systems, Faculty of Technical Sciences Čačak, Serbia. Electrical resistivity was measured by the four-point method [18, 19], by passing dc current through the sample. The same method was used in nonisothermal and isothermal conditions. Due to the low resistivity of aluminium, measurement of electrical resistivity is very difficult (see for instance Ref. [12], [20]), i.e. small cross-section of the sample is necessary. A reliable contact between the leads and the ribbon has to be ensured during thermoelectric measurements. The TEMF of the alloy was measured by the compensation method having a sensitivity of 10^{-5} V [21]. Thermoelectrical processing was performed in a protecting argon atmosphere.

3. Results and discussion

3.1 Thermoelectric measurements

The diagram in Fig. 1 shows the temperature dependence of the relative change in electrical resistivity of the investigated alloy.

Fig. 1 illustrates that thermal stabilization of the structure involves an abrupt decline in electrical resisivity due to a change in electronic energy states. An inflection point is observed in curves (a) and (c), suggesting two stages (processes) of structural arrangement. These changes are more pronounced for the thinner ribbon (curve c), indicating a higher degree of structural disorder. During casting process, the speed of the copper rotating disk was higher for ribbons of 35 μm in thickness, which led to a higher quenching rate of the molten alloy and, hence, an increased degree of structural disorder. Curve (b) representing the second annealing shows an almost linear dependence typical for the crystal structure. The same qualitative behaviour was recorded for second heating run of 35 μm thick sample (not shown here), as well as for AlSi10Mg crystalline sample (curve d on Fig. 1) investigated by Brandt and Neuer [12].

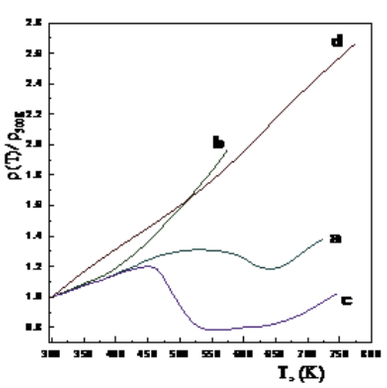

Figure1. *Temperature dependence of the relative change in electrical resistivity: first heating (d = 60 μm), b) second heating (d=60 μm), c) first heating (d=35 μm), d) crystalline AlSi10Mg, data from Ref. [12]*

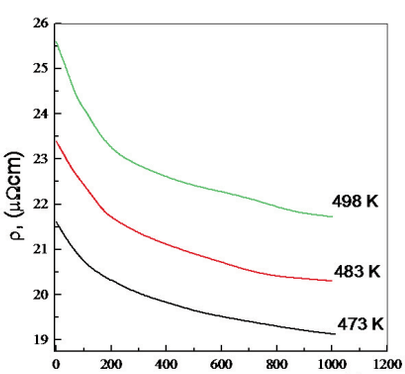

Figure 2. *Isothermal changes in electrical resistivity (ribbon sample thickness d = 60 μm), at temperatures T_1=473 K, T_2=483 K and T_3=498 K.*

Table 1. *The chemical composition of investigated AlSi10Mg alloy.*

Si	Fe	Cu	Mn	Mg	Zn	Other	Al
9.0-10.0	0.6	0.1	0.05	0.45-0.6	0.05	0.15	Ballance

The diagram in Fig. 2 shows isothermal changes in electrical resisivity at temperatures T_1 = 473 K, T_2 = 483 K and T_3 = 498 K for a 60 µm thick ribbon.

The dependence obtained *ρ (τ)* was found to be of an exponential form (relaxation time approximation for isothermal changes of electrical resistivity [22]):

$$\rho(\tau) = \rho_O \cdot \exp(-k\tau) \quad (1)$$

where ρ_0 – initial electrical resisivity at isotherm recording temperature, k - rate constant. After logarithming the experimentally obtained dependences *ρ(τ)*, Fig. 2, linear dependences *ln ρ(τ)* during the first τ_1=140 s, τ_2=120 s and τ_3=120 s were obtained for temperatures T_1 = 473 K, T_2 = 483 K and T_3 = 498 K, respectively (Fig. 3).

This confirms that a rapid activation controlled kinetic process is the first stage of structural relaxation. During the process, fine interatomic movements occur, with atoms progressing from a less stable state to a more stable state. Concurrently, the density of both chaotically distributed dislocations and dot defects was found to decrease, causing a reduced internal microstrain level, i.e. overall structural relaxation.

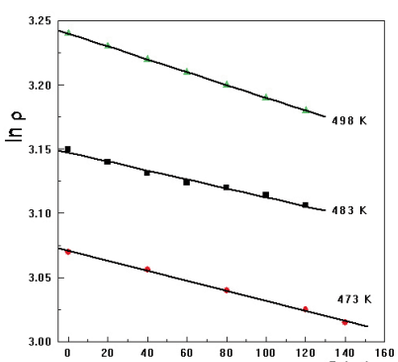

Figure 3. *Dependence of ln ρ on time τ at temperatures T_1 = 473 K, T_2 = 483 K and T_3 = 498 K.*

The increase in isothermal annealing temperature reduces the duration of that stage in the process and induces an increase in the rate constant of the stage. From the equation (1) it can be obtained:

$$k = \frac{\Delta \ln \rho}{\Delta \tau} \quad (2)$$

In the second interval of time 160 s <τ_1'< 700 s ; 140 s <τ_2'< 600 s, and 140 s <τ_3'< 500 s, a linear dependence of electrical resistivity ρ on $\tau^{1/2}$ was observed for the three isothermal annealing temperatures (Fig. 4). The dependence obtained confirms that the second stage of structural relaxation is a slow diffusion process, involving intercavity mass transport and free volume reduction.

The rate constant of second stage was calculated from equation:

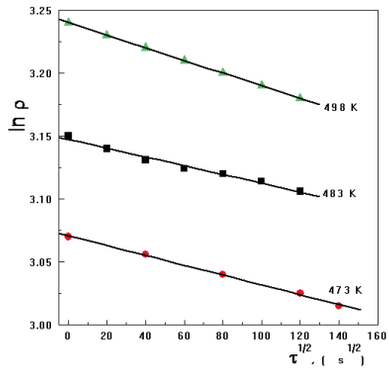

Figure 4. *Dependence of ρ as a function of $\tau^{1/2}$ for samples annealed at temperatures T_1= 473 K, T_2= 483 K and T_3= 498 K.*

$$k' = \frac{\Delta \rho}{\Delta \tau^{1/2}} \quad (3)$$

The diagram in Fig. 5 shows the dependence of ln k and ln k' on 1000/T at temperatures T_1, T_2 and T_3. It can be noticed that the structural relaxation increases with increasing temperature.

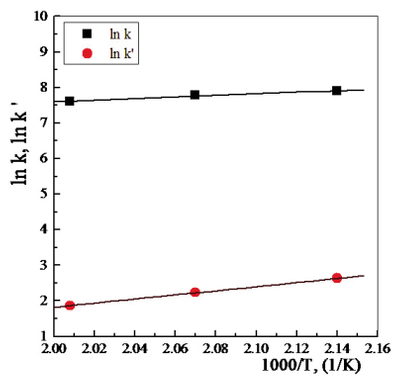

Figure 5. *Dependence of ln k and ln k' on 1000/T.*

Activation energies E_a for both stages of structural relaxation were determined from the slope Δ *ln k*/Δ (*1/T*), following the Arrhenius' equation written in the form [23]:

$$E_a = R_g \frac{\Delta \ln k}{\Delta\left(\frac{1}{T}\right)} \quad (4)$$

where R_g is gas constant. Obtained kinetic parameters are presented in Table 2.

Table 2. *Kinetic parameters of the structural relaxation of metastable AlSi10Mg alloy*

T, (K)	k, (10^{-4} s^{-1})	k', (10^{-2} s^{-1})	E_a, (kJ/mol)	E_a', (kJ/mol)
473	3.75	7.2		
483	4.2	10.8	19	48
498	5	16		

3.2 Analysis of TEMF measurement results

Dependence of TEMF - ε upon temperature ΔT ($\Delta T = T\text{-}T_r$, $T_r = 273$ K), is given by the equation $\varepsilon = \alpha \cdot \Delta T$ where α is thermopower (Seebeck coefficient) defined as:

$$\alpha = \frac{k}{2e}\left(\frac{n_1}{n_2} - \frac{n_2}{n_1}\right) \quad (5)$$

where: k- Boltzmann constant, e- electron charge, n_1-free electron state density at Fermi level in copper, n_2-free electron density at Fermi level in the metastable AlSi10Mg alloy [21]. The diagram in Fig. 6 shows TEMF measurement results for the thermocouple metastable AlSi10Mg alloy – Cu wire during successive heating cycles. For the sake of clarity, the figure presents results only for first four heating cycles.

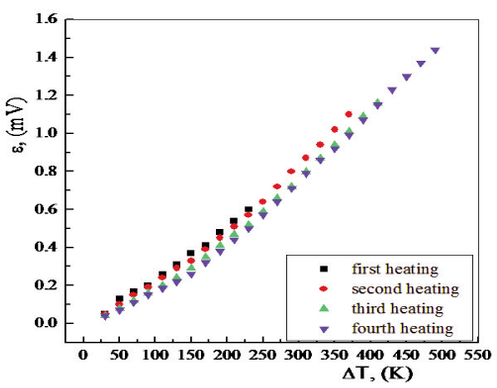

Figure 6. *Dependence of the TEMF of the thermocouple AlSi10Mg ribbon - Cu wire: I - first heating up to 503 K, II - second heating up to 643 K,III - third heating up to 683 K, IV-fourth heating up to 763 K.*

The results obtained from Fig. 6 show that each heating resulted in a decrease in thermopower. For each measurement, thermopower was determined in the temperature range of $\Delta T = 90$ K to $\Delta T = 110$ K, their values being $\alpha_I = 3$ μV/K, $\alpha_{II} = 2.7$ μV/K, $\alpha_{III} = 2.5$ μV/K, $\alpha_{IV} = 2$ μV/K, respectively. Determination of thermopower at 380 K was made due to the assumption that, the electron state density in the alloy does not change upon each successive heating (see curves a, b and c in Fig. 1 up to 380 K), up to this temperature. Therefore, changes in thermopower during the succeeding heating cycle are induced by structural changes in the alloy during the preceding heating cycle.

Starting from Eq. (5), relative changes in electron state density of the ribbon sample as compared to electron state density at Fermi level in copper can be calculated (for details see Ref. [15]). The decrease in thermopower confirms that electron density at the Fermi level increases during each heating cycle as induced by thermal treatment:

$\Delta n_{2I}/n_1 = 8.3\%$ $\Delta n_{2II}/n_1 = 16.7\%$

$\Delta n_{2III}/n_1 = 25.3\%$ $\Delta n_{2IV}/n_1 = 30$ %.

The decrease in thermopower after each heating cycle is the result of the metastable state relaxation of the alloy. Heat treatment caused a decrease in the density of chaotically distributed dislocations and microstrain level in the alloy, leading to improved overlapping between 2p and 3s electron subshells of neighbouring Al atoms, thereby causing an increase in n_2 electron density of states at the Fermi level in the alloy. Upon two successive heat treatments up to 763 K, thermopower remains constant during these heating cycles.

A complete correlation was observed between the present results and those regarding measurement of the temperature dependence of electrical resisivity. Therefore, the abrupt decline in electrical resisivity in the temperature range of 450 K to 550 K (for d = 35 μm) and 550 K to 650 K (for d = 60 μm) was induced by the increase in both the mean free path of electrons and the electron density of states at the Fermi level.

4. Conclusions

Thermoelectric measurements showed that structural stabilization of the metastable AlSi10Mg alloy takes place during heating. Structural changes were found to be most intense in the 450 K to 650 K temperature range.

Isothermal measurements of the changes in electrical resisivity revealed two stages of structural relaxation: a rapid activation-controlled kinetic process and a diffusion process. Thermopower measurements, performed after successive heat treatments of the same alloy sample, showed an increase in the electron density of states at the Fermi level after each heating cycle. Therefore, the abrupt decline in electrical resisivity during heating is associated with increases in the mean free path of electrons, electron density and electron density of states at the Fermi level.

Acknowledgment

This work was supported by the Ministry of Education and Science, Republic of Serbia (Project OI 172057 Controlled synthesis, structure and properties of multifunctional materials).

References

[1] A. Inoue, K. Hashimoto, "Amorphous and Nanocrystalline Materials: Preparation, Properties, and Applications", Springer, Berlin, New York, 2001.

[2] S. Djukić, V. Maričić, A. Kalezić-Glišović, L. Ribić-Zelenović, S. Randjić, N. Mitrović, N. Obradović, Sci. Sintering 43 (2) (2011) 175-182.

[3] F. E. Luborsky, Amorphous Metallic Alloys, Butterworths, London, 1983.

[4] A. Inoue, Mater. Sci. Eng. A 304-306 (2001) 1-10.

[5] A. Maričić, D. Minić, V. Blagojević, A. Kalezić-Glišović, D. Minić, Intermetallics 21 (1) (2012) 45-49.

[6] A. Inoue, "Bulk Amorphous Alloys: Practical Characteristics and Applications", Trans Tech Publications Ltd, Zurich, 1999.

[7] K. Matusita, S. Sakka, J. Non-Cryst. Sol. 38 -39 (2) (1980) 741-746.

[8] A. Dalvi, A.M. Awasthi, S. Bharadwaj, K. Shahi, Mater. Sci. Eng. B 103 (2) (2003) 162-169.

[9] D. M. Minić, A. Gavrilović, P. Angerer, D. G. Minić, A. Maričić, J. Alloys Compd. 476 (1-2) (2009) 705-709.

[10] H. Chiriac, A. Inoue, F. Barariu, V. Nagacevschi, Mater. Sci. Eng. A 226-228 (1997) 650-653.

[11] Y. Birol, J. Alloys Compd. 513 (2012) 150-153.

[12] R. Brandt, G. Neuer, Int. J. Thermophys. 28 (5) (2007) 1429-1446.

[13] M. I. Daoudi, A. Triki, A. Redjaimia, J. Therm. Anal. Calorim. 104 (2011) 627-633.

[14] M. I. Daoudi, A. Triki, A. Redjaimia, C. Yamina, Thermochim. Acta 577 (2014) 5-10.

[15] M. Stipcich, A. Cuniberti, V. Noseda Grau, J. Alloys Compd. 542 (2012) 248-252.

[16] H. Beck, H. J. Guntherodt, Glassy Metals II, Springer-Verlag, Berlin, 1983.

[17] M. Vončina, P. Mrvar, J. Medved, RMZ – Materials and Geoenvironment, 52 (3) (2006) 621-633.

[18] N. S. Mitrović, S. N. Kane, S. Roth, A. Kalezić-Glišović, C. Mickel, J. Eckert, J. Min. Metall. Sect. B-Metall. 48 (2) (2012) 319-324.

[19] N. S. Mitrović, S. N. Kane, P.V. Tyagi, S. Roth, J. Magn. Magn. Mater. 320 (20) (2008) e792-e796.

[20] M. Petrič, S. Kostelic, P. Mrvar, J. Min. Metall. Sect. B-Metall. 49 (3) (2013) 279-283.

[21] A. Maričić, M. Spasojević, A. Kalezić-Glišović, L. Ribić-Zelenović, S. Djukić, N. Mitrović, Sens. Actuators A: Phys. 174 (2012) 103-106.

[22] J. Wolny, R. Kokoszka, J. Soltys, P. Barta, J. Non.-Cryst. Solids Vol. 113 (2-3) (1989) 171-177.

[23] A. Kalezić-Glišović, A. Maričić, N. Mitrović, R. Simenunović, M. Spasojević, J. Optoelectron. Adv. Mater. 10 (3) (2008) 504-507.